Available online at www.sciencedirect.com
ScienceDirect
Earth and Planetary Science Letters 256 (2007) 554–566
EPSL
www.elsevier.com/locate/epsl

Hydrothermal venting of greenhouse gases triggering Early Jurassic global warming

Henrik Svensen [a,*], Sverre Planke [a,b], Luc Chevallier [c], Anders Malthe-Sørenssen [a], Fernando Corfu [d], Bjørn Jamtveit [a]

[a] *Physics of Geological Processes (PGP), University of Oslo, PO Box 1048 Blindern, 0316 Oslo, Norway*
[b] *Volcanic Basin Petroleum Research (VBPR), Oslo Research Park, 0349 Oslo, Norway*
[c] *Council for Geoscience, PO Box 572 Bellville 7535, Cape Town, South Africa*
[d] *Department of Geosciences, University of Oslo, PO Box 1047 Blindern, 0316 Oslo, Norway*

Received 20 November 2006; received in revised form 31 January 2007; accepted 2 February 2007
Available online 13 February 2007
Editor: R.W. Carlson

Abstract

The climate change in the Toarcian (Early Jurassic) was characterized by a major perturbation of the global carbon cycle. The event lasted for approximately 200,000 years and was manifested by a global warming of ~6 °C, anoxic conditions in the oceans, and extinction of marine species. The triggering mechanisms for the perturbation and environmental change are however strongly debated. Here, we present evidence for a rapid formation and transport of greenhouse gases from the deep sedimentary reservoirs in the Karoo Basin, South Africa. Magmatic sills were emplaced during the initial stages of formation of the Early Jurassic Karoo Large Igneous Province, and had a profound influence on the fate of light elements in the organic-rich sedimentary host rocks. Total organic carbon contents and vitrinite reflectivity data from contact aureoles around the sills show that organic carbon was lost from the country rocks during heating. We present data from a new type of geological structures, termed breccia pipes, rooted in the aureoles within the shale of the Western Karoo Basin. The breccia pipes are cylindrical structures up to 150 meters in diameter and are mainly comprised of brecciated and baked black shale. Thousands of breccia pipes were formed due to gas pressure build-up during metamorphism of the shales, resulting in venting of greenhouse gases to the Toarcian atmosphere. Mass balance calculations constrained by new aureole data show that up to 1800 Gt of CO_2 was formed from organic material in the western Karoo Basin. About 15 times this amount of CO_2 (27,400 Gt) may have formed in the entire basin during the intrusive event. U–Pb dating of zircons from a sill related to many of the pipes demonstrates that the magma was emplaced 182.5±0.4 million years ago. This supports a causal relationship between the intrusive volcanism, the gas venting, and the Toarcian global warming.

Keywords: climate change; Toarcian; carbon cycle perturbation; contact metamorphism; degassing; breccia pipes; the Karoo Basin

1. Introduction

The geological record shows that abrupt changes in the atmospheric concentration of greenhouse gases have occurred throughout the Earth's history (*e.g.*, [1–7]).

* Corresponding author. Tel.: +47 22 85 61 11, +47 93053870 (Mobile); fax: +47 22 85 51 01.
E-mail address: hensven@fys.uio.no (H. Svensen).

0012-821X/$ - see front matter © 2007 Elsevier B.V. All rights reserved.
doi:10.1016/j.epsl.2007.02.013

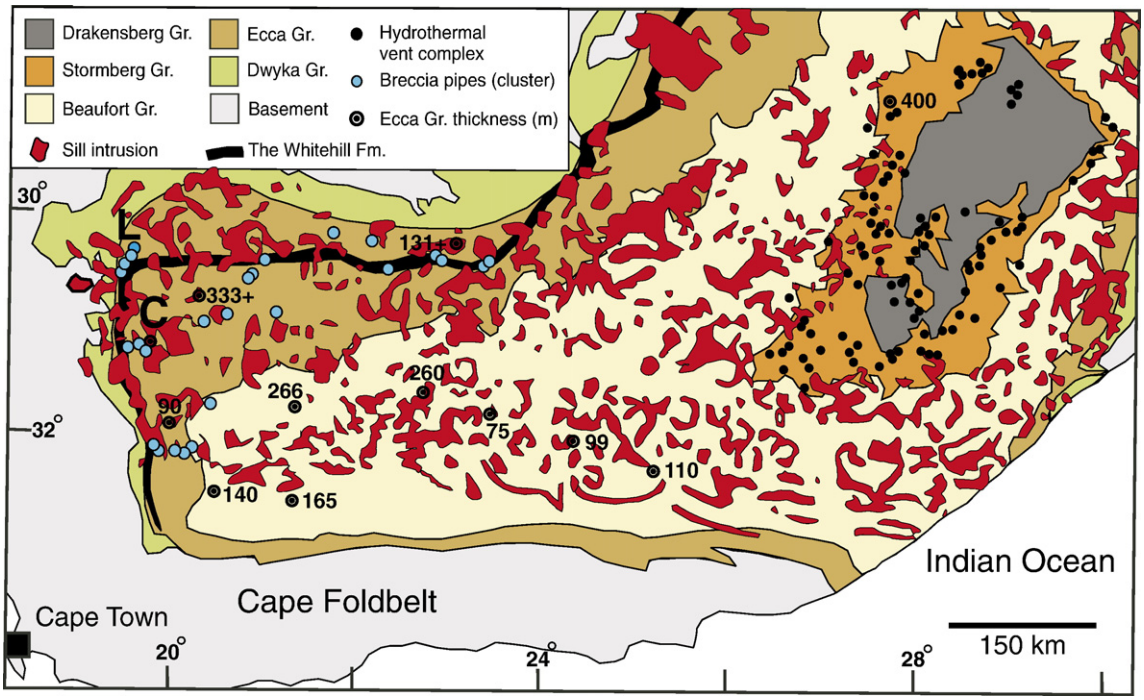

Fig. 1. Distribution of hydrothermal vent complexes and breccia pipes in the Karoo Basin, South Africa. About 390,000 km^2 of the currently exposed Karoo Basin contains dolerite intrusions emplaced in sedimentary rocks. Phreatic hydrothermal vent complexes are mainly confined to outcrops in the Stormberg Group sediments located near the Early Jurassic paleo-surface [25], whereas the breccia pipes are confined to the Ecca and lowermost Beaufort groups. Note that the symbols for the breccia pipes represent pipe clusters. This study is primarily based on data from the Loriesfontein (L) and Calvinia (C) areas.

Moreover, more than six episodes of major climatic and environmental perturbations correlate with the timing of Large Igneous Provinces (LIPs) (*e.g.*, [5–7]). Release of several thousand gigatons of isotopically light carbon as greenhouse gases from sedimentary successions to the atmosphere has been proposed as a cause of warm periods at the Permo–Triassic boundary (~251 million years ago (Ma)), in the Toarcian (~183 Ma/Early Jurassic), and in the initial Eocene (~55 Ma) [2–4,8–11]. The resulting climate changes are extensively documented by chemical proxy data from sedimentary rocks, commonly demonstrating 5–10 °C global warming lasting a few hundred thousand years, accompanied by anoxic conditions in the oceans and mass extinctions. The exact relationship between LIPs and climate perturbations is however poorly understood, and the geological processes responsible for rapid formation and transport of greenhouse gases from the huge sedimentary reservoir to the atmosphere are debated (*e.g.*, [12–14]).

Melting of marine gas hydrates has for the last decade been the favored climatic trigger among many geoscientists (*e.g.*, [2,8,15]), but recent estimates of the present day hydrate reservoir questions its possible contribution [16]. The role of LIP lava degassing has been downplayed due to the long duration (>500 000 yr) of lava emplacement and the relatively "heavy" carbon isotopic composition of magmatic CO_2. Nevertheless, lava degassing is considered to have been a key mechanism for the end-Permian and Toarcian environmental changes (*e.g.*, [5,7,18–20]). New data from the Northeast Atlantic have shown that LIPs and abrupt climate changes may be causally connected by the formation of volcanic basins. Svensen et al. [10] proposed that the Paleocene Eocene Thermal Maximum (PETM) was triggered by rapid formation and transport of greenhouse gases from metamorphic aureoles around igneous sill intrusions in the Vøring and Møre basins offshore mid-Norway. Furthermore, McElwain et al. suggested in 2005 [4], based on new paleobotanical data, that metamorphism of coal beds around sills in Antarctica and subsequent release of CO_2 is a possible analogous mechanism for the Toarcian warming event. In this paper, we present new evidence for a causal relationship between intrusive magmatism in the Karoo Basin, contact metamorphism, carbon degassing, and the Toarcian global warming and carbon cycle perturbation.

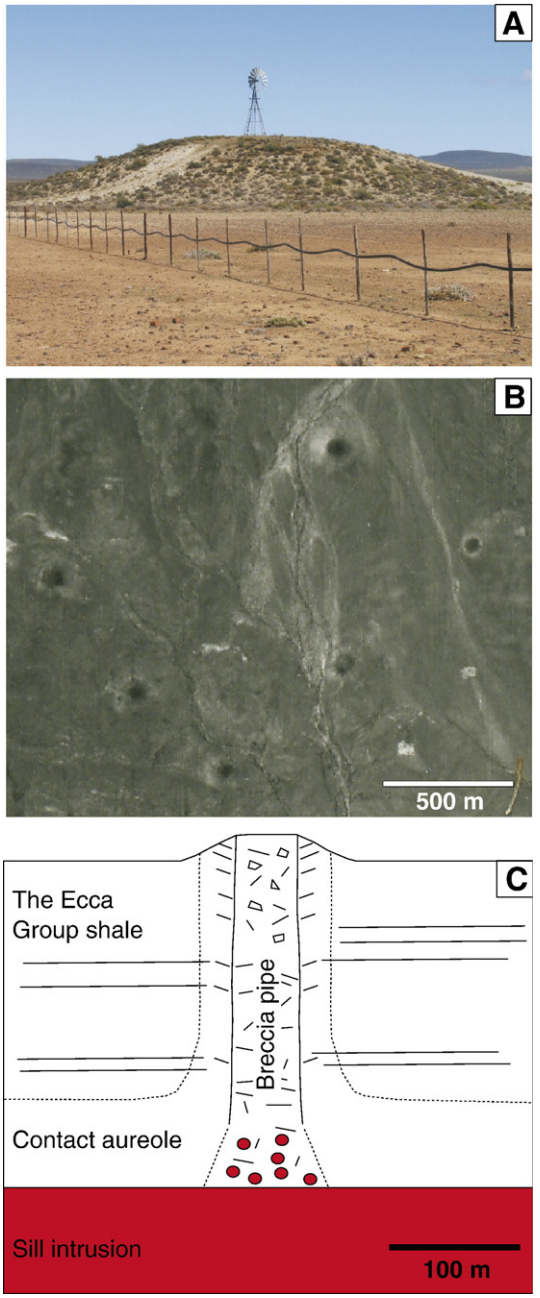

Fig. 2. Breccia pipes in the western Karoo Basin. A) Typical outcrop of a breccia pipe in the Loriesfontein area. The rim of the pipe comprises metamorphic and disturbed sedimentary strata, whereas the pipe centre is filled with brecciated and metamorphosed sediments. B) Aerial photo covering a few of the breccia pipes in the Loriesfontein area. Note the black fill of the pipes (breccia), and the surrounding bleached metamorphic sediments. C) Schematic cross section of the relationship between sill, contact metamorphic aureole, and breccia pipe. The area with the red spots in the contact metamorphic aureole symbolizes sediment-dolerite interactions. (For interpretation of the references to colour in this figure legend, the reader is referred to the web version of this article.)

2. Sills and breccia pipes in the Karoo Basin

The Karoo Basin is well suited to study processes initiated by intrusive volcanism and contact metamorphism as the entire basin succession is currently exposed in South Africa. The foreland basin is filled by up to 8 km thick Carboniferous to Early Jurassic sedimentary strata (Fig. 1) [21]. Large volumes of mafic magma intruded the basin in the Early Jurassic, about 183 Ma [22,23]. These magmatic sills and dykes were emplaced as a part of the Karoo–Ferrar large igneous province, originally extending across southern Africa, Antarctica, Argentina and Tasmania. A number of basin-wide organic-rich marine shales are present in the lower part of the Karoo Basin, in particular the Whitehill and Prince Albert formations of the Ecca Group (Figs. 1 and 3). The Ecca Group is well exposed in the western parts of the basin, where it is intruded by up to 120-m thick planar sills. The sills heated adjacent sedimentary strata, leading to metamorphic reactions in the aureoles and the expansion of pore fluids. High overpressure resulted in phreatic eruptions and the formation of hundreds of hydrothermal vent complexes presently exposed in the central parts of the Karoo Basin (Fig. 1) [24,25].

An outstanding feature of the western Karoo Basin is the presence of breccia pipes associated with sills and contact metamorphic aureoles (Figs. 1 and 2). The breccia pipes are sub-vertical cylindrical structures that cut through sedimentary strata. They are generally between 20 and 150 m in diameter, and are filled with brecciated and metamorphic shale. We have mapped more than 20 clusters of breccia pipes within a 50,000 km^2 large area where the Ecca Group sediments outcrop in the western Karoo (Fig. 1). Based on the interpretation of aerial photos, we estimate that the total number of breccia pipes currently exposed is on the order of several thousand.

3. Methods

We have studied more than 25 boreholes drilled in and around breccia pipes from the western Karoo Basin. Detailed analyses were focused on the Loriesfontein and Calvinia areas (labelled L and C in Fig. 1). Cores from the three boreholes, one stratigraphic and two from breccia pipes, were logged and sampled at the core library at the Council for Geoscience, Pretoria.

Bulk rock powders were analyzed for total organic carbon (TOC) and vitrinite reflectance at Applied Petroleum Technology, Kjeller, Norway. Acid treatment

of the powders was done to quantify the content of inorganic carbon (lower than 0.2 wt.% in all samples). The TOC was estimated using a Rock–Eval 6 instrument during oxidation to CO/CO_2 in the temperature range 300–650 °C. Carbon dioxide released between 650 and 850 °C during pyrolysis is interpreted as originating from graphite oxidation. For vitrinite reflectance measurements, powders were treated with hydrochloric and hydrofluoric acid before kerogen embedment in epoxy. Polished slabs were analyzed on a Zeiss MPM 03 photometer microscope equipped with an oil objective. The reflectance measurements were calibrated against several standards. At least 20 measurements were made per sample, and the results are reported as percent reflectivity in oil (% Ro). The quality of the analyses depends on the abundance and type of vitrinite, particle size and surface quality, and the uncertainty is typically below 10%.

U–Pb analyses were carried out by the ID-TIMS (isotope dilution thermal ionization) at the University of Oslo on handpicked crystals of zircon ($ZrSiO_4$) and baddeleyite (ZrO_2) from sample G39974-596m. All crystals were abraded before analysis, except for baddeleyite because of its scarcity and small size. Chemical separation on anion exchange resin was done for all fractions except the three weighing less than 1 μg, which were measured without further processing. Use of a mixed ^{235}U–^{205}Pb–^{202}Pb spike permitted an internal normalization for the fractionation of

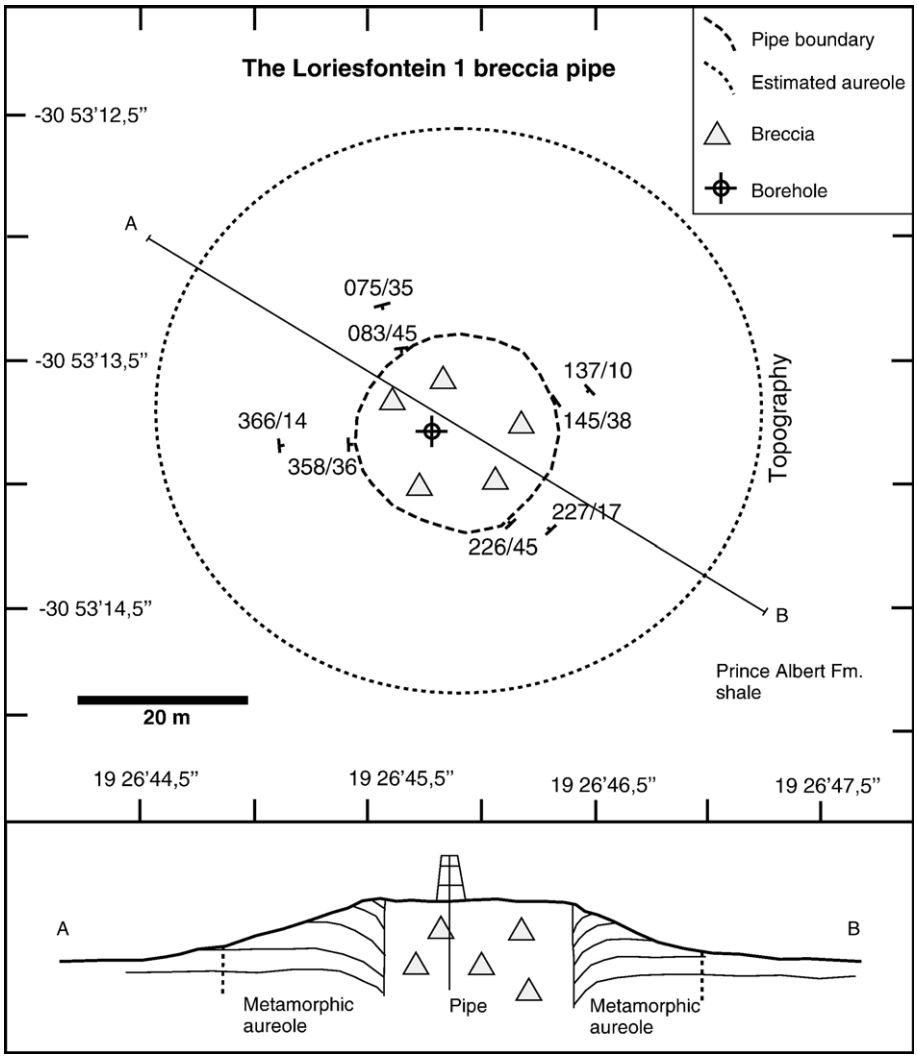

Fig. 3. Simplified map of the breccia pipe from Fig. 2A. The pipe is circular with a sharp transition to the dipping (up to 45°) and metamorphic country rocks (Tierberg Formation). The borehole in the centre was drilled for ground water purposes, and penetrates sedimentary breccias.

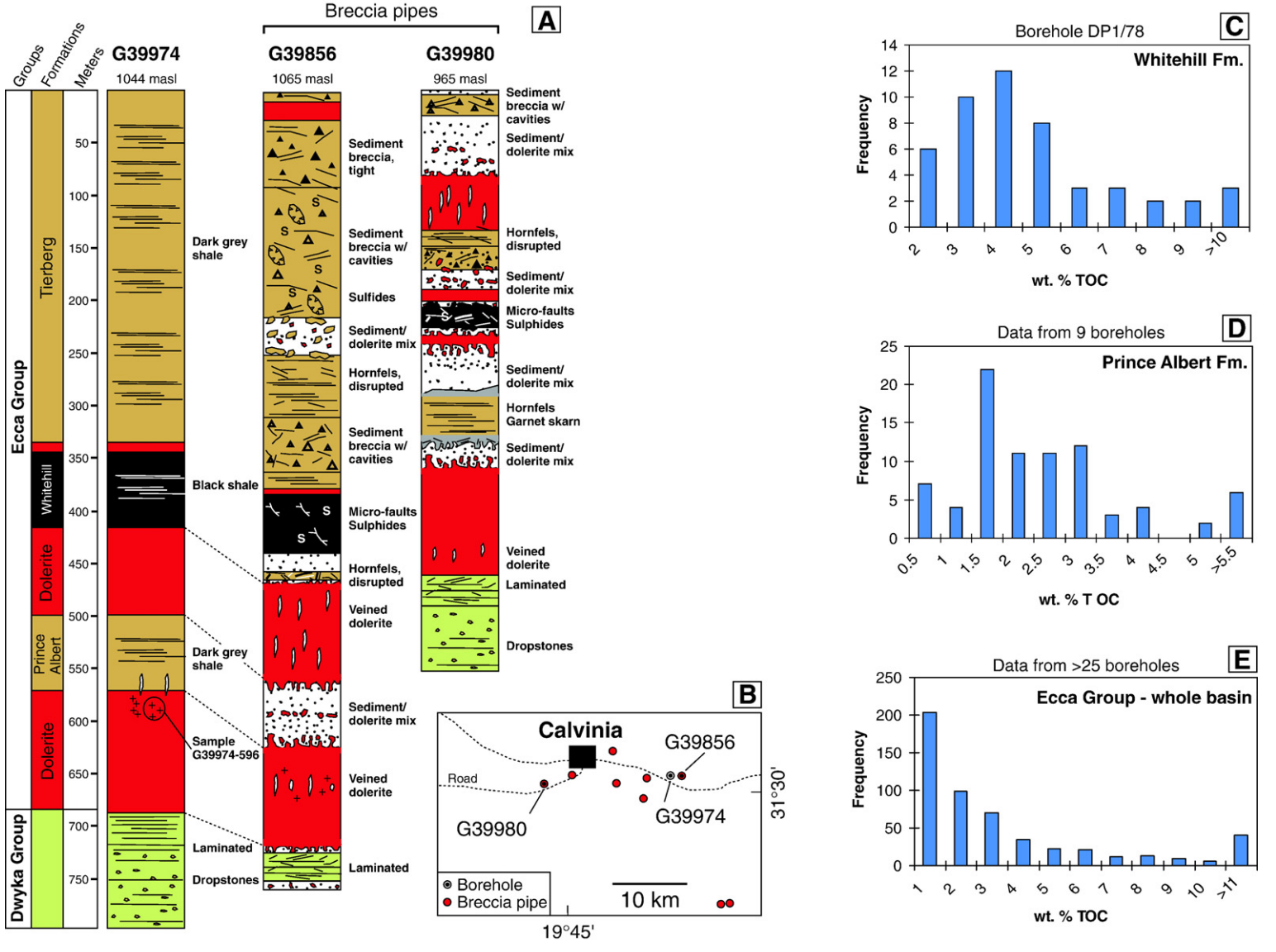

Fig. 4. Stratigraphic borehole and breccia pipe logs. A) The log from the stratigraphic borehole (G39974) forms the basis for the contact aureole carbon mass balance presented in this paper. Two of the studied boreholes are from breccia pipes (G39856 and G39980) and comprise baked and brecciated sediments together with doleritic magmatic rocks. B) Index map showing the locations of the Calvinia area boreholes. C–E) Compilation of total organic carbon (TOC) contents of the Ecca Group shale from the Karoo Basin, based on Faure and Cole [45], Cole and McLachlan [37], and Rowsell and De Swardt [36].

Pb. See [26] for analytical procedures. The data are presented in Table 1 using decay constants from Jaffey et al. [27]. Uncertainties represent 2σ.

4. Results

4.1. Breccia pipes and metamorphism

We have carried out detailed field and borehole studies of two areas with a high density of breccia pipes: The Calvinia and Loriesfontein areas (Fig. 1). About 430 breccia pipes have been mapped from aerial photos in the Loriesfontein area within the black shale of the Ecca Group. These pipes are typically spaced at 0.5 to 1 km. Field work demonstrate that the pipes are more or less circular in horizontal section with sharp contacts to the surrounding sediments (Figs. 2 and 3). Moreover, the adjacent sedimentary strata are inward-dipping. This is a common feature of piercement structures in sedimentary basins with vertical mass transport (*e.g.*, [25, 28,29]). The breccia pipes have been a target for ground water drilling in the Calvinia area, and up to 1016 m long cores have been recovered (Fig. 4) [30]. We have conducted a detailed petrographic and geochemical study of one stratigraphic core (G39974) and two breccia pipe cores (G39856 and G39980). The pipes are characterized by more or less *in situ* brecciation and metamorphism of organic-rich layers from the Ecca Group (Fig. 4). The borehole logs clearly show that the breccia pipes are rooted in contact aureoles with baked black shale and mixtures of sediments and dolerite. Generally, the breccia pipes contain metamorphic shale from the Ecca Group, and show evidence of sediment–dolerite interactions near the root zones (Fig. 4). The rock types of the breccia pipes can be divided in three main groups (Fig. 5): 1) Intervals with dolerite–sediment mixtures, commonly present close to the sills. 2) Contact metamorphic breccia with no visible porosity, typically present at the Prince Albert and Whitehill Formations levels. 3) High porosity breccias, mostly within the uppermost Ecca Group, with abundant mineralization (pyrite, chalcopyrite, quartz, and metals like Ag and Au)

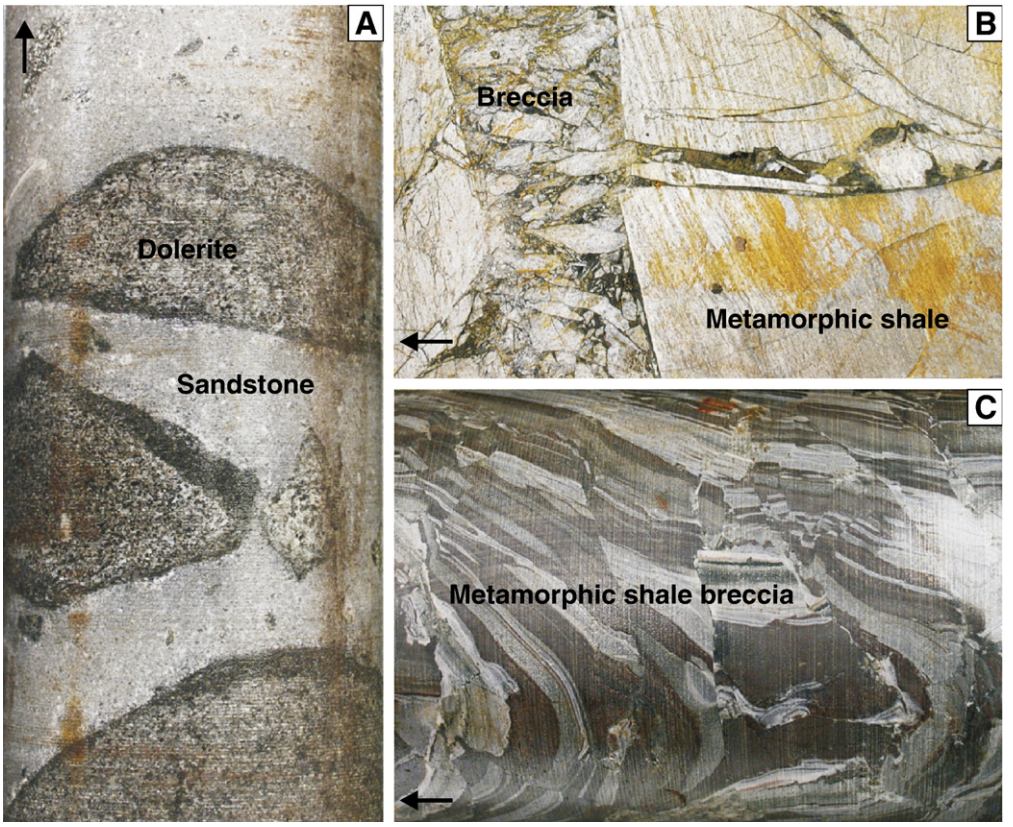

Fig. 5. Rock types in the breccia pipes, here with examples of core photos from borehole G39980. See Fig. 4B for location. A) Dolerite–sandstone mixture at 338 m depth. B) High porosity breccia in metamorphic Tierberg Formation shale at 20 m depth. C) Tight breccia in metamorphic Whitehill Formation, 216 m. The cores are 7 cm in diameter, and the arrows point in the upward direction of the borehole.

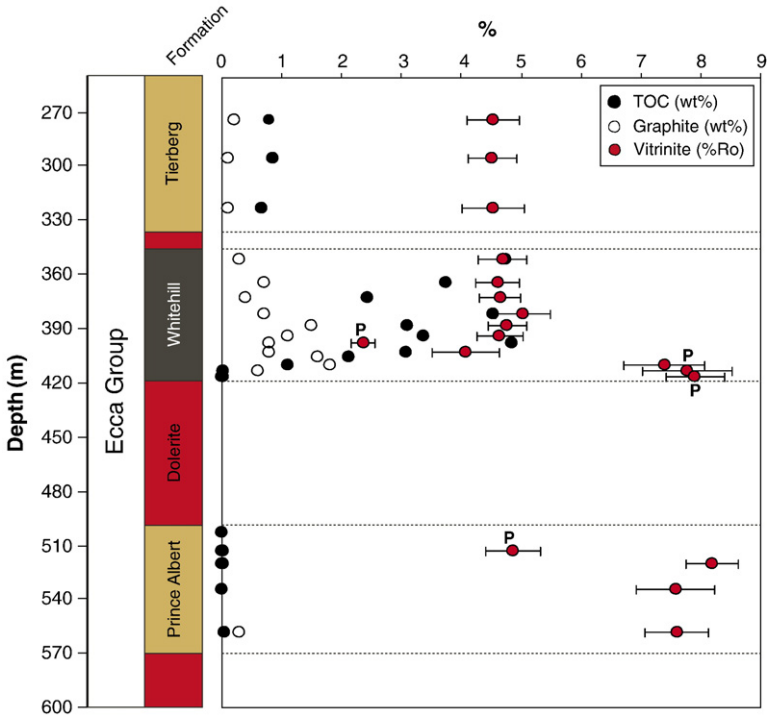

Fig. 6. Carbon loss in metamorphic shale. Stratigraphy and geochemistry of borehole G39974. Three dolerite sills (red) are present in the borehole, and the vitrinite reflectance and the total organic carbon (TOC) values document the heating effect on the sediments. The TOC is virtually zero in the Prince Albert Formation, whereas the Whitehill Formation shows a significant reduction in TOC immediately above the sill intrusion. Part of the TOC reduction in the Whitehill Formation contact aureole can be explained by transformation to graphite. The whole Ecca Group sequence in the boreholes has been heated beyond the temperature of gas generation (>1.5% Ro). Note that the quality of the vitrinite reflectivity measurements close to the sill intrusions is poor (labelled "P"). (For interpretation of the references to colour in this figure legend, the reader is referred to the web version of this article.)

in cavities. We have not been able to locate breccia pipes at higher stratigraphic levels than the Beaufort Group due to the present day erosional level. However, hydrothermal vent complexes are numerous in the upper stratigraphy of the basin (the Stormberg Group), and could have acted as degassing outlets for thermogenic gas [24,25].

The shale in the stratigraphic borehole G39974 is interlayered with several sills (Fig. 4). Vitrinite reflectance measurements of metamorphic shale and breccia adjacent to the sills show the severe thermal effects of the intruded magma on the organic material (Fig. 6). Furthermore, the metamorphic minerals in both the pipes and the stratigraphic borehole include garnet, demonstrating high temperature metamorphism. The metamorphic shale in G39974 shows vitrinite reflectance values of 2.4 to 8.2% Ro (Fig. 6). These values are well above the threshold value of 1.5% Ro corresponding to temperature regimes where gas is normally produced, and demonstrate a very high degree of transformation of the original organic material [31]. The contact aureole in the Whitehill Formation shows a typical correlation between increasing % Ro values and decreasing bulk rock TOC contents. The total organic carbon (TOC) values in the aureoles of the sills in G39974 show that virtually all organic carbon is missing from the 70-m thick Prince Albert Formation, whereas the Whitehill Formation has experienced a significant reduction in organic carbon (Fig. 6). The organic carbon was likely transformed to isotopically light CO_2, CH_4, and possibly other hydrocarbons during contact metamorphism (*cf*. [31,32]), and subsequently lost from the aureole rocks. Original TOC values in the Prince Albert Fm. are commonly between 1.5 and 4.5 wt.% (Fig. 4D), and may locally reach >5 wt.%. Fig. 6 shows that some of the organic carbon was transformed to graphite, and thus remained in the shale throughout metamorphism. The amount of graphite is insignificant in the Prince Albert and Tierberg formations, whereas the Whitehill Formation contains up to 1.5 wt.% graphite (a TOC/graphite ratio of 2). During high temperature contact

Table 1
U–Pb ID-TIMS data for zircon and baddeleyite

Characteristics*	Weight[a]	U	Th/U[b]	Pb_c[c]	$^{206}Pb/^{204}Pb$[d]	$^{207}Pb/^{235}U$[e]	±2σ	$^{206}Pb/^{238}U$[e]	±2σ	ρ	$^{207}Pb/^{206}Pb$[e]	±2σ	$^{206}Pb/^{238}U$[e]	±2σ	$^{207}Pb/^{235}U$[e]	±2σ	$^{207}Pb/^{206}Pb$[e]	±2σ
	(μg)	(ppm)		(pg)			(abs)		(abs)			(abs)			(age in Ma)			
G39974-596m																		
Z eu lp [9]	<1	>7370	2.27	1.1	11876	0.19725	0.00054	0.028753	0.000071	0.93	0.04975	0.00005	182.7	0.4	182.8	0.5	183.5	2.4
Z eu lp [11]	6	4283	3.05	2.9	16125	0.19713	0.00052	0.028724	0.000068	0.96	0.04977	0.00004	182.6	0.4	182.7	0.4	184.5	1.7
Z eu lp (cr tu) [9]	13	3031	2.51	4.4	15919	0.19670	0.00047	0.028660	0.000061	0.96	0.04978	0.00004	182.2	0.4	182.3	0.3	184.6	1.7
Z eu lp [9]	7	2096	2.51	2.0	13240	0.19740	0.00079	0.028733	0.000112	0.91	0.04983	0.00009	182.6	0.7	182.9	0.6	186.9	4.0
Z eu lp (incl) [9]	10	1716	3.24	1.6	19097	0.19698	0.00045	0.028671	0.000058	0.95	0.04983	0.00004	182.2	0.3	182.6	0.3	187.0	1.8
B fr NA [7]	7	103	0.06	1.5	903	0.19472	0.00177	0.028415	0.000092	0.48	0.04970	0.00040	180.6	0.6	180.7	1.5	181.1	19
B fr NA [7]	6	43	0.06	1.3	381	0.19509	0.00408	0.028530	0.000115	0.41	0.04960	0.00097	181.3	0.7	181.0	3.5	176.1	45

* Z = zircon; B = baddeleyite; eu = euhedral; lp = long prismatic (*l*/*w*=>4); cr = cracks; tu = turbid spots; incl = inclusions; [*N*] = number of grains in fraction; fr = fraction; NA = non abraded.
[a] Weight and concentrations are known to be better than 10%, except for those near the *ca*. 1 μg limit of resolution of the balance.
[b] Th/U model ratio inferred from 208/206 ratio and age of sample.
[c] Pb_c = total common Pb in sample (initial+blank).
[d] Raw data corrected for fractionation and blank.
[e] Corrected for fractionation, spike, blank and initial common Pb; error calculated by propagating the main sources of uncertainty.

metamorphism, graphite would further react to CO_2 and CH_4 [33].

4.2. U–Pb age of the sill intrusion and the breccia pipes

The zircons from sample G39974-596m occur predominantly as long-prismatic crystals dominated by {100} and {101} crystal faces. The crystals are commonly broken and contain inclusions, mainly of biotite. They contain very high amounts of U (1700 to over 7400 ppm) and have the high Th/U typical of zircon in mafic rocks (Table 1). The total common Pb is in the range of the blank except for turbid grains that had as much as 4.4 pg common Pb. The five analyses plot on or slightly to the right of the Concordia curve but have uniform $^{206}Pb/^{238}U$ ages of 182.7 to 182.2 Ma, which are reflected in the Concordia age of 182.5±0.4 Ma (Fig. 7). Calculation of the latter includes the decay constant error, and even then the MSWD of concordance is only 1.9. This deviation of the analyses towards too high $^{207}Pb/^{235}U$ ages has been a noticeable feature of many high-precision U–Pb data sets in the past and has been documented recently by Schoene et al. [34], who suggest that the behaviour may be related to a slightly erroneous decay constant. The baddeleyite data plot below the zircon data points suggesting that the crystals have lost some lead.

5. Discussion

5.1. Methane production potential

Estimates of carbon production potential in an intruded sedimentary basin require information about contact aureole volume (area A * thickness h), and the amount of carbon in wt.% transferred to methane or carbon dioxide, F_C. The total mass of carbon, W_C, produced in contact aureoles is:

$$W_C = F_C * A * h * \rho * S,$$

where ρ is the rock density (2400 kg/m^3). Our parameter A is measured from the area with mapped breccia pipes, corresponding to 650 km^2 in the Loriesfontein area and 50,000 km^2 in the western Karoo Basin. The thickness h of the aureole can be estimated by the TOC and the vitrinite reflectivity data for the metamorphic sediments. The parameter S is a measure of the shape of the aureole as reflected by the TOC profile, such that $S=1$ for an aureole with no gradient in the TOC loss, *i.e.*, a box-

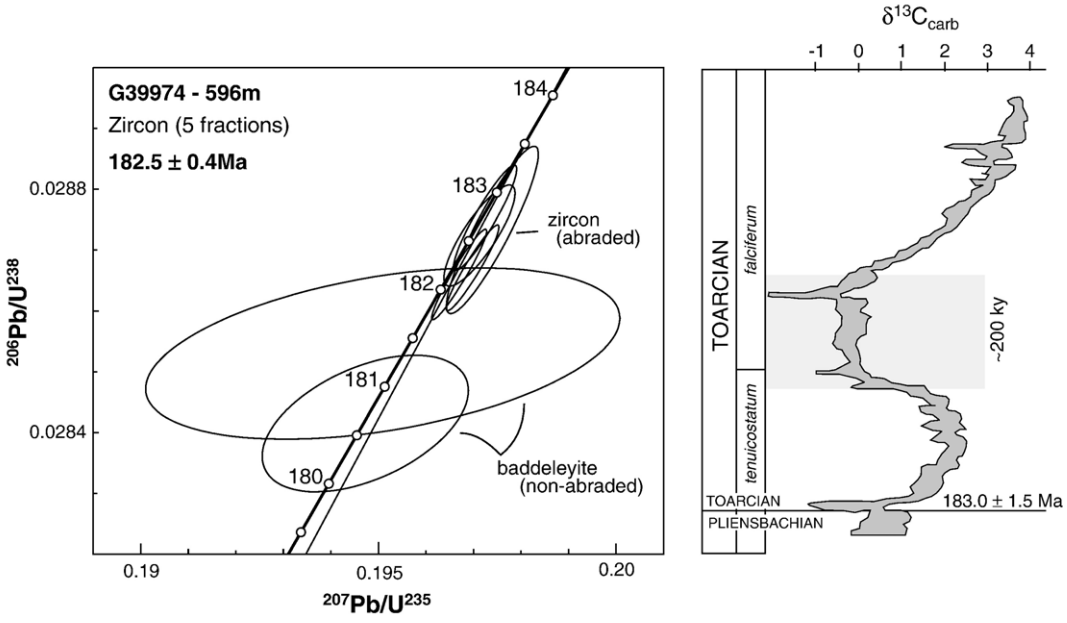

Fig. 7. Dating of breccia pipes and the Torcian global warming. A) U–Pb concordia plot for sample G39974-596m. The five zircon analyses plot on or slightly to the right of the Concordia curve but have uniform $^{206}Pb/^{238}U$ ages of 182.7 to 182.2 Ma, which are reflected in the Concordia age of 182.5±0.4 Ma. The baddeleyite data plot below the zircon data points, suggesting that the crystals have lost some lead. The raw data are presented in Table 1. B) The Toarcian global climate change as defined by a negative carbon isotope excursion, here from a dataset of bulk carbonate isotope data from Peniche, Portugal (modified from [38]). The negative carbon isotope excursion can be explained by a global perturbation of the carbon cycle, with massive addition of ^{12}C-enriched carbon to the atmosphere and oceans [2–4,38].

shaped aureole, and $S=0.5$ for an aureole with a linear profile of TOC loss towards the intrusive contact. For more complex TOC profiles of the contact aureole, other factors for S must be used. The total mass of carbon produced, W_C, can be converted to equivalents of methane ($=W_C * 1.34$) and carbon dioxide ($=W_C * 3.66$). The produced thermogenic methane has a depleted carbon isotope ratio ($\delta^{13}C=-35$ to -50‰) [31].

Compilation of characteristic total organic carbon (TOC) values from the Karoo Basin shows that unmetamorphosed shale has 2–8 wt.% TOC in the Whitehill Formation and 0.5–4 wt.% TOC in the Prince Albert Formation (Fig. 4C–E). Thus the gas generation potential is significant. Also, the actual aureole data from borehole G39974 supports that a significant fraction of the organic matter was transformed to carbon gas during metamorphism, as increasing % Ro values correlate with decreasing TOC contents. Furthermore, we can use these data to calculate the W_C.

5.2. Production and venting of greenhouse gases in the Loriesfontein area

The mass of produced greenhouse gases in the metamorphic aureoles in the Loriesfontein area can be calculated from the demonstrated loss of TOC in the Ecca Group. For borehole G39974, h is 70 m for the Prince Albert Formation ($F_C=1.5$–3.5, $S=1$) and 70 m for the Whitehill Formation ($F_C=4$–5, $S=0.5$). The values for the shape parameter S are approximated from the TOC and vitrinite data shown in Fig. 6.

We may extrapolate the contact aureole depletion in TOC recorded in borehole G39974 to the 650 km^2 area where breccia pipes are mapped in the Loriesfontein area, and thus estimate the regional carbon loss during metamorphism. For the Loriesfontein area estimates, we have assumed that the sill emplacement levels and aureole thicknesses are as in G39974. Consequently, when extrapolating the TOC loss, we find that between 3.8 and 6.6 Gt carbon is missing from the Prince Albert and Whitehill Formations. This is equivalent to 5.1–8.8 Gt CH_4 or 14–24 Gt CO_2. The fate of the generated gas is directly linked to the breccia pipes, which formed as a consequence of the metamorphic aureole processes. Here, a low permeability resulted in considerable pressure build-up during gas generation [24], whereas subsequent hydrofracturing ultimately led to breccia pipe formation and vigorous sub aerial gas eruptions. Note that the mass of carbon gases vented to the atmosphere in the Loriesfontein area alone is of the same order of magnitude as the annual anthropogenic carbon release of about 23 Gt CO_2 [35].

We use the results from the Loriesfontein and Calvinia areas to extrapolate for what happened in the ~50,000 km^2 western Karoo Basin with breccia pipes, using the same aureole parameters as from the Calvinia and Loriesfontein areas. The extrapolation indicates that between 294 and 504 Gt of carbon was transformed to greenhouse gases during contact metamorphism. Recalculated to gas equivalents, this corresponds to 394–675 Gt CH_4 or 1076–1845 Gt CO_2. It should be noted that this estimate is conservative and that the known variations in regional aureole thickness and background TOC could increase the gas generation potential 2–3 times (*i.e.*, to between 3700 and 5500 Gt CO_2).

5.3. Basin scale gas generation

The basin scale sill emplacement in the Ecca Group organic-rich sediments caused widespread gas generation, and we need to consider the basin as a whole for understanding the full implications of the metamorphism for the Toarcian climate. We use an approximation where contact aureoles and carbon loss are assumed to be present throughout the present-day area with sills in carbon-rich sediments (390,000 km^2). The thickness of the Ecca Group varies considerably on a basin scale, and there is limited information available about the full extent of contact metamorphism and the details of TOC profiles. Nevertheless, maturity parameters and diagenetic mineralogy show that the sill emplacement had a significant effect on the Ecca Group sediments on a basin-wide scale [36,37], thus supporting widespread gas generation in contact aureoles.

We assume a basin scale aureole thickness of 100–200 m, but in contrast to the Loriesfontein case we use this as a bulk property regardless of the thicknesses and TOC contents of the individual formations. The TOC loss is assumed to be 2–5 wt.% in the 100 m aureole case and 2–4 wt.% in the 200 m case. The chosen TOC background values are based upon the data from G39974 and an extensive database from the Karoo Basin (Fig. 4C–E). Using this approach, the potential for gas generation in aureoles is between 1870 and 7490 Gt C or the equivalent 6850 and 27,400 Gt CO_2. This estimate does not include the contribution from metamorphism of coal beds in the Ecca Group of the Eastern Karoo Basin or the metamorphism around sills in the Beaufort and Stormberg formations. Furthermore, the lower value of 6850 Gt CO_2 is only 3.7 times higher than the western Karoo Basin estimate, and accordingly an under-estimation since the area under consideration is eight times bigger.

5.4. Relationship to the Toarcian carbon cycle perturbation

Proxy data demonstrate a major perturbation of the carbon cycle during the Pliensbachian–Toarcian, about 183 Ma. The global extent of the perturbation has recently been questioned [14,12], but new data from fossil wood fragments supports that the carbon cycle perturbation represents an episode of global warming during the Toarcian [38]. The climate change lasted for about 200,000 yr, although some authors argue for duration of at least 520,000 yr [20]. Furthermore, the event was characterized by a global warming of ~6 °C, anoxic conditions in the oceans, and extinction of marine species [1,3,17,18,39].

Age constraints on the breccia pipe formation are given by radiometric dating of zircons from a pegmatite interval in the lowermost sill in G39974, defining a U–Pb Concordia age of 182.5±0.4 Ma (Fig. 7). The timing of breccia pipe formation and gas release from the Karoo Basin is thus restricted to the late Pliensbach or early Toarcian (the stage boundary is placed at 183.0±1.5 Ma) [40]. Moreover, the dolerite age is indistinguishable from the lower Toarcian interval where the negative carbon excursion and the oceanic anoxic event are located (*tenuicostatum* and *falciferum* ammonite zones) [2,4]. Our results are in agreement with the 183.7±0.6 Ma U–Pb age obtained from a sill in the Eastern Karoo Basin [41]. Most of the radiometric dating of igneous rock from the Karoo Basin is either on lavas (*i.e.*, with limited relevance for the timing of breccia pipe formation) or on sills using the relatively low precision Ar/Ar method. Published Ar/Ar ages show a spread of about 6 million years for the few sills dated so far from the Karoo Basin [22]. Furthermore, we emphasize that sill emplacement and breccia pipe formation likely happened on a much shorter timescale than the >6 million years of lava eruptions in Southern Africa [42]. Supporting geological evidence includes a) the virtual absence of sill/dyke cutting relationships in the field, b) sills are connected in a saucer-like manner throughout the basin [30,43], c) sills may extend for hundreds of kilometers and must have been emplaced rapidly since they cool on a timescale of 100–1000 yr, d) the total volume of melt in the sills is very small compared to the volumes of the lava flows, and e) the lava eruptions from the Karoo province slightly post dated the hydrothermal venting [25]. Still, the main phase of lava eruptions in South Africa had a short duration (a few hundred thousand years) and likely contributed to the perturbation of the Toarcian carbon cycle [22].

Independent support for the hypothesis of a carbon degassing-origin of the Toarcian global warming comes from the use of fossil leafs as a CO_2 proxy. McElwain et al. attributed a rapid atmospheric CO_2 increase to contact metamorphism of coal in Antarctica [4]. If vented to the atmosphere, the gas produced in the Antarctic part of the volcanic province would clearly add to the effect of the degassing through the breccia pipes. To conclude, the sedimentary basin degassing scenario as a mechanism to perturb the carbon cycle can account for the triggering of the Toarcian event. The degassing should furthermore be taken into consideration when discussing the other hypotheses for the Toarcian, such as increased organic productivity, gas hydrate dissociation and oceanographic changes [1,2,12–15,44].

6. Conclusions

The new geological, geochemical and geochronology data represent evidence for large scale carbon gas venting in the Early Jurassic. It is likely that the many thousands of breccia pipes formed within the 200,000 yr time span of the Toarcian global warming. Our data show that nearly 2000 Gt CO_2 could have been produced from the Ecca Group in the western Karoo Basin. This is a conservative estimate considering the total area with sill intrusions in organic rich shale, which has a production potential of at least 27,400 Gt CO_2. The venting from the Karoo Basin could consequently have acted as the main trigger for the Toarcian carbon cycle perturbation. The Toarcian greenhouse would have been further accelerated by the metamorphism of coal deposits in Antarctica, long term lava degassing from the Karoo–Ferrar province, astronomical climate forcing [3], and by feedback mechanisms such as melting of gas hydrates [2,4].

Our new data clearly tie the Toarcian carbon cycle perturbation to the Karoo LIP and the volcanic Karoo Basin. Our hypothesis highlights the importance of the emplacement environment of LIPs in causing global environmental climate changes. Ultimately, an understanding of the triggering mechanism and consequences of previous climatic changes driven by carbon gas emissions is highly relevant for predicting the consequences of current anthropogenic carbon emissions, as these events are likely of similar magnitude and duration.

Acknowledgements

This study was supported by grants from the Norwegian Research Council to B.J., A.M-S., and H.S. through a Centre of Excellence and PetroMaks grant to PGP. We would like to thank D. Cole, J. Marsh, and R. Opperman for

discussions about the geology of the Karoo Basin, and the Council for Geoscience in South Africa (handled by David Motloi) for access to cores. We thank S.P. Hesselbo and A.D. Saunders for constructive reviews.

References

[1] H.C. Jenkyns, The Early Toarcian (Jurassic) anoxic event: stratigraphic, sedimentary and geochemical evidence, Am. J. Sci. 288 (1988) 101–151.

[2] S.P. Hesselbo, et al., Massive dissociation of gas hydrate during a Jurassic oceanic anoxic event, Nature 406 (2000) 392–395.

[3] D.B. Kemp, A.L. Coe, A.S. Cohen, L. Schwark, Astronomical pacing of methane release in the Early Jurassic period, Nature 437 (2005) 396–399.

[4] J.C. McElwain, J. Wade-Murphy, S.P. Hesselbo, Changes in carbon dioxide during an oceanic anoxic event linked to intrusion into Gondwana coals, Nature 435 (2005) 479–482.

[5] V.E. Courtillot, P.R. Renne, On the ages of flood basalt events, C. R. Geosci. 335 (2003) 113.

[6] R.B. Stothers, Flood basalts and extinction events, Geophys. Res. Lett. 20 (1993) 1399–1402.

[7] P.B. Wignall, Large igneous provinces and mass extinctions, Earth-Sci. Rev. 53 (2001) 1–33.

[8] G.R. Dickens, J.R. O'Neil, D.K. Rea, R.M. Owen, Dissociation of oceanic methane hydrate as a cause of the carbon isotope excursion at the end of the Paleocene, Paleoceanography 10 (1995) 965–971.

[9] R.A. Berner, Examination of hypotheses for the Permo–Triassic boundary extinction by carbon cycle modeling, PNAS 99 (2002) 4172–4177.

[10] H. Svensen, S. Planke, A. Malthe-Sørenssen, B. Jamtveit, R. Myklebust, T. Eidem, S.S. Rey, Release of methane from a volcanic basin as a mechanism for initial Eocene global warming, Nature 429 (2004) 542–545.

[11] J.C. Zachos, et al., Rapid acidification of the ocean during the Peleocene–Eocene thermal maximum, Science 308 (2005) 1611–1615.

[12] P.B. Wignall, J.M. McArthur, C.T.S. Little, A. Hallam, Methane release in the Early Jurassic period, Nature 441 (2006) E5.

[13] D.B. Kemp, A.L. Coe, A.S. Cohen, L. Schwark, Methane release in the Early Jurassic period, Nature 441 (2006) E5–E6.

[14] B. van de Schootbrugge, J.M. McArthur, T.R. Bailey, Y. Rosenthal, J.D. Wright, K.G. Miller, Toarcian oceanic anoxic event: an assessment of global causes using belemnite C isotope records, Paleoceanography 20 (2005), doi:10.1029/2004PA001102.

[15] D.J. Beerling, M.R. Lomas, D.R. Gröcke, On the nature of methane gas–hydrate dissociation during the Toarcian and Aptian oceanic anoxic events, Am. J. Sci. 302 (2002) 28–49.

[16] A.V. Milkov, Global estimates of hydrate–bound gas in marine sediments: how much is really out there? Earth-Sci. Rev. 66 (2004) 183.

[17] J. Pálfy, P.L. Smith, J.K. Mortensen, Dating the end-Triassic and Early Jurassic mass extinctions, correlative large igneous provinces, and isotopic events, Spec. Pap. - Geol. Soc. Am. 356 (2002) 523–532.

[18] J. Pálfy, P.L. Smith, Synchrony between Early Jurassic extinction, oceanic anoxic event, and the Karoo–Ferrar flood basalt volcanism, Geology 28 (2000) 747–750.

[19] S.L. Kamo, G.K. Czamanske, Y. Amelin, V.A. Federenko, D.W. Davis, V.R. Trofimov, Rapid eruption of Siberian flood–volcanic rocks and evidence for coincidence with the Permian–Triassic boundary and mass extinction at 251 Ma, Earth Planet. Sci. Lett. 214 (2003) 75–91.

[20] E. Mattioli, B. Pittet, R. Bucefalo Palliani, H.-J. Röhl, A. Schmid-Röhl, E. Morettini, Phytoplankton evidence for the timing and correlation of paleoceanographical changes during the early Toarcian anoxic event (Early Jurassic), J. Geol. Soc. (Lond.) 161 (2004) 685–693.

[21] O. Catuneanu, P.J. Hancox, B.S. Rubidge, Reciprocal flexural behaviour and contrasting stratigraphies: a new basin development model for the Karoo retroarc foreland system, South Africa, Basin Res. 10 (1998) 417–439.

[22] R.A. Duncan, P.R. Hooper, J. Rehacek, J.S. Marsh, A.R. Duncan, The timing and duration of the Karoo igneous event, Southern Gondwana, J. Geophys. Res. 102 (1997) 18127–18138.

[23] L. Chevallier, A.C. Woodford, Morpho-tectonics and mechanism of emplacement of the dolerite rings and sills of the western Karoo, South Africa, S. Afr. J. Geol. 102 (1999) 43–54.

[24] B. Jamtveit, H. Svensen, Y. Podladchikov, S. Planke, Hydrothermal vent complexes associated with sill intrusions in sedimentary basins, Spec. Publ. - Geol. Soc. Lond. 234 (2004) 233–241.

[25] H. Svensen, B. Jamtveit, S. Planke, L. Chevallier, Structure and evolution of hydrothermal vent complexes in the Karoo Basin, South Africa, J. Geol. Soc. (Lond.) 163 (2006) 671.

[26] F. Corfu, U–Pb age, setting, and tectonic significance of the anorthosite–mangerite–charnockite–granite-suite, Lofoten–Vesterålen, Norway, J. Petrol. 45 (2004) 1799–1819.

[27] A.H. Jaffey, K.F. Flynn, L.E. Glendenin, W.C. Bentley, A.M. Essling, Precision measurement of half-lives and specific activities of ^{235}U and ^{238}U, Phys. Rev., C Nucl. Phys. 4 (1971) 1889–1906.

[28] S. Planke, H. Svensen, M. Hovland, DA. Banks, B. Jamtveit, Mud and fluid migration in active mud volcanoes in Azerbaijan, Geo Mar. Lett. 23 (2003) 258–268.

[29] S. Planke, T. Rassmussen, S.S. Rey, R. Myklebust, Seismic characteristics and distribution of volcanic intrusions and hydrothermal vent complexes in the Vøring and Møre basins, in: T. Dore, B. Vining (Eds.), Petroleum Geology: North-West Europe and Global Perspectives. Proceedings of the 6th Petroleum Geology Conference, Geological Society Publishing House, London, 2005, pp. 833–844.

[30] A.C. Woodford, L. Chevallier (Eds.), Hydrogeology of the main Karoo Basin: current knowledge and research needs, Water Research Commission Report, vol. TT 179/02, 2002.

[31] J.M. Hunt, Petroleum Geochemistry and Geology, W.H. Freeman, San Francisco, 1996.

[32] P.A. Meyers, B.R.T. Simoneit, Effects of extreme heating on the elemental and isotopic compositions of an Upper Cretaceous coal, Org. Geochem. 30 (1999) 299–305.

[33] J.A.D. Connolly, B. Cesare, C–O–H–S fluid composition and oxygen fugacity in graphitic metapelites, J. Metamorph. Geol. 11 (1993) 379–388.

[34] B. Schoene, J.L. Crowley, D. Condon, M.D. Schmitz, S.A. Bowring, Reassessing the uranium decay constants for geochronology using ID-TIMS U–Pb data, Geochim. Cosmochim. Acta 70 (2006) 426–445.

[35] IPCC (Intergovernmental Panel on Climate Change), Climate Change 2001: The Scientific Basis, IPCC, Geneva, 2001.

[36] D.M. Rowsell, A.M.J. De Swardt, Diagenesis in Cape and Karoo sediments, South Africa and its bearing on their hydrocarbon potential, Trans. Geol. Soc. S. Afr. 79 (1976) 81–145.

[37] D.I. Cole, I.R. McLachlan, Oil shale potential and depositional environment of the Whitehill Formation in the main Karoo Basin, Council for Geoscience (South Africa) Report, vol. 1994–0213, 1994.

[38] S.P. Hesselbo, H.C. Jenkyns, L.V. Duarte, L.C.V. Oliveira, Carbon-isotope record of the Early Jurassic (Toarcian) Oceanic Anoxic Event from fossil wood and marine carbonate (Lusitanian Basin, Portugal), Earth Planet. Sci. Lett. 253 (2007) 455–470.
[39] C.T.S. Little, M.J. Benton, Early Jurassic mass extinction: a global long-term event, Geology 23 (1995) 495–498.
[40] F.M. Gradstein, et al., A Geologic Time Scale 2004, Cambridge University Press, 2004.
[41] J. Encarnación, T.H. Fleming, D.H. Elliot, H.V. Eales, Synchronous emplacement of Ferrar and Karoo dolerites and the early breakup of Gondwana, Geology 24 (1996) 535.
[42] F. Jourdan, et al., Karoo large igneous province: brevity, origin, and relation to mass extinction questioned by new $^{40}Ar/^{39}Ar$ age data, Geology 33 (2005) 745–748.
[43] A. Malthe-Sørenssen, S. Planke, H. Svensen, B. Jamtveit, Formation of saucer-shaped sills, Geological Society of London, Special Publications, vol. 234, 2004, pp. 215–227.
[44] H.C. Jenkyns, D.R. Gröcke, S.P. Hesselbo, Nitrogen isotope evidence for water mass denitrification during the early Toarcian (Jurassic) oceanic anoxic event, Paleoceanography 16 (2001) 593–603.
[45] K. Faure, D. Cole, Geochemical evidence for lacustrine microbial blooms in the vast Permian Main Karoo, Paraná, Falkland Islands and Huab basins of southwestern Gondwana, Palaeogeogr. Palaeoclimatol. Palaeoecol. 152 (1999) 189–213.